Guided-mode-resonance coupled localized surface plasmons for dually resonance enhanced Raman scattering sensing

Zheng Wang[†, a, b], Chao Liu[†, a], Erwen Li[c], Swapnajit Chakravarty[d], Xiaochuan Xu[d], Alan X. Wang*[, c], D.L. Fan*[, a, e], and Ray T. Chen*[,a,b,d]

[†]These authors equally contributed to this work.

[a]Materials Science and Engineering Program, Texas Materials Institute, The University of Texas at Austin, Austin, TX USA 78712;
[b]Dept. of Electrical and Computer Engineering, The University of Texas at Austin, 10100 Burnet Rd., MER 160, Austin, TX USA 78758;
[c]School of Electrical Engineering and Computer Science, Oregon State University, Corvallis, OR, 97331, USA;
[d]Omega Optics, Inc., 8500 Shoal Creek Blvd., Bldg. 4, Suite 200, Austin, TX USA 78757;
[e]Dept. of Mechanical Engineering, the University of Texas at Austin, Austin, TX USA 78712;

ABSTRACT

Raman scattering spectroscopy is a unique tool to probe vibrational, rotational, and other low-frequency modes of a molecular system and therefore could be utilized to identify chemistry and quantity of molecules. However, the ultralow efficient Raman scattering, which is only $1/10^9 \sim 1/10^{14}$ of the excitation light due to the small Raman scattering cross-sections of molecules, have significantly hindered its development in practical sensing applications. The discovery of surface-enhanced Raman scattering (SERS) in the 1970s and the significant progress in nanofabrication technique, provide a promising solution to overcome the inherent issues of Raman spectroscopy. It is found that In the vicinity of nanoparticles and their junctions, the Raman signals of molecules can be significantly improved by an enhancement factor as high as 10^{10}, due to the ultrahigh electric field generated by the localized surface plasmons resonance (LSPR), where the intensity of Raman scattering is proportional to the $|\mathbf{E}|^4$. In this work, we propose and demonstrate a new approach combining LSPR from nanocapsules with densely assembled silver nanoparticles (NC-AgNPs) and guide-mode-resonance (GMR) from dielectric photonic crystal slabs (PCSs) for SERS substrates with robustly high performance.

Keywords: Surface-Enhanced Raman Scattering, Photonic Crystal Slabs, Guided-Mode Resonance, Raman Nanosensor

1. INTRODUCTION

Raman scattering was independently observed by Indian [1] and Soviet [2] scientists in 1928. It offers an approach for people to probe vibrational, rotational, and other low-frequency modes in a molecular system and therefore could be utilized to identify chemistry and quantity of molecules [3]. However, the virtual quantum state nature determines the relatively small Raman scattering cross-section, which results in the intensity of Raman scattering of only $1/10^9 \sim 1/10^{14}$ of the input excitation [4]. The ultra-low efficient Raman scattering has greatly hindered its development in practical sensing applications [5]. In the 1970s, the observation of enhanced Raman spectra on the roughened silver surface [6] and discovery of surface-enhanced Raman scattering (SERS) [7, 8] effect offered a promising solution to overcome the inherent issues of Raman spectroscopy. However, back at that time, the fabrication technique could hardly deliver effective SERS substrates. Since the 1990s, the development of SERS has been considerably benefited from the emergence of nanotechnology, and plenty of nanostructures have been invented [9]. The metallic nanostructures offer

* wang@eecs.oregonstate.edu; dfan@austin.utexas.edu; chenrt@austin.utexas.edu

Plasmonics in Biology and Medicine XIV, edited by Tuan Vo-Dinh, Joseph R. Lakowicz, Proc. of SPIE
Vol. 10080, 1008003 · © 2017 SPIE · CCC code: 1605-7422/17/$18 · doi: 10.1117/12.2253383

"hot spots", which are nanoscale confinements of electromagnetic fields [10]. In the vicinity of "hot spots", localized surface plasmons resonance (LSPR) could induce greatly enhanced electromagnetic field, and the intensity of Raman scattering could be substantially amplified by an enhancement factor (EF) as high as 10^{10} due to the $|\mathbf{E}|^4$ enhancement [11-13]. By such high EFs, the single-molecule-detection capability can be achieved [14-16]. With the ultra-high sensitivity, SERS technique has shown great potential in multiple civilian and military applications such as early cancer diagnostic[17-19], environmental pollution monitoring [20-22], and chemical warfare agent detection [23-25].

Recently, guided-mode resonance (GMR) in photonic crystal slabs (PCSs), which has been extensively studied in filter applications [26-29], has drawn great attention for its potential application in the enhancement of Raman signals. Guided-mode resonance can substantially boost localized electric fields (E) in the vicinity of PCSs due to their efficient trapping of the light. The effect can readily enhance Raman signals of molecules due to the $|\mathbf{E}|^4$ dependence [30-32]. Thanks to the Fano resonance principle in photonic crystals and materials, local electromagnetic filed enhancement also can be realized in uniform dielectric photonic crystal slabs which do not require precise placement of designed nanoentities onto the substrates [33]. In this paper, we propose and demonstrate an approach which utilizes GMR from a PCS and LSPR from nanocapsules with densely assembled silver nanoparticles (NC-AgNPs) to build plasmonic-photonic hybrid nanosensors. Here each individual nanocapsule (NC) is an assembly of densely packed "hot spots," which provides a constant and stable enhancement in addition to the existing SERS effect. It is not only the simple, rapid, and cost-effective bottom-up chemical synthesis process but also the high density "hot spots" with ideal gap size [34] between the silver (Ag) nanoparticles (NPs) on NCs that makes the NC-AgNPs an ideal plasmonic SERS substrates [35-38]. Nile blue, which is a standard dye for SERS research, is selected for this study. In our experiment, the NC-AgNPs sitting on PCS gains an additional 4.67 times enhancement and the total EF as high as 1.8×10^9 has been achieved.

2. DESIGN AND NUMERICAL SIMULATION

For this study, a t = 230 nm thick low-stress Si_3N_4 layer on 0.5mm silica serves as the device layer. We first designed the PCS via Stanford stratified structure solver (S^4), which is a frequency domain linear Maxwell's equations solver for layered periodic structures[39]. The rigorous coupled-wave analysis (RCWA) algorithm enables S^4 to be a fast, precise, and effective approach with numerous experimental demonstrations in multiple research areas[40-50]. For the PCS which contains rectangular air hole array, its two characteristic parameters that period p of air hole array and the diameter d of air holes are shown in Fig. 1a. By virtue of the periodicity of PCS, we only need to perform simulations in a single cell. Figure 1b shows the simulated structure with a Cartesian coordinate. In our simulations, all geometrical parameters are normalized to the p. Figure 1c shows the simulated distributions of the time averaged electric field enhancement $|\overline{\mathbf{E}}|/|\overline{\mathbf{E}_0}|$ at y = 0 and z = 0 planes at the desired wavelength 633 nm, which is the center wavelength of our excitation laser. Here $|\overline{\mathbf{E}_0}|$ is the time averaged electric field intensity of the incident excitation. The black lines in Fig. 1d represents the boundaries between different materials.

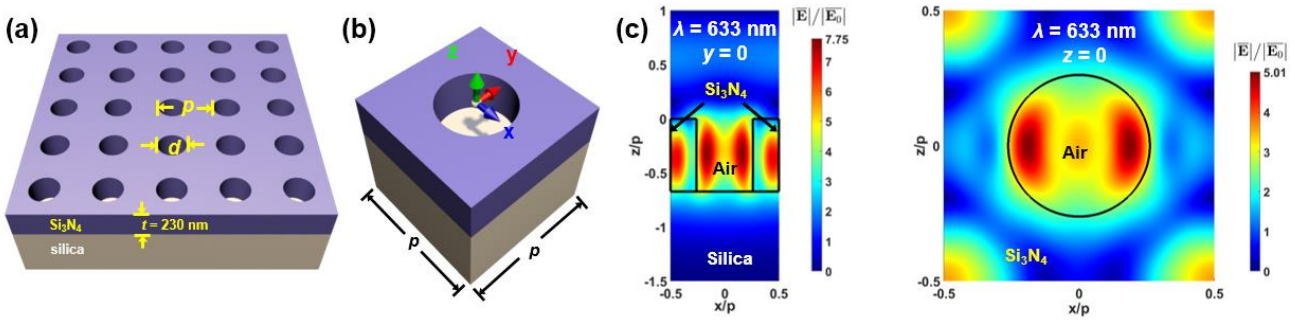

Fig. 1. Schematics of the PCS (a) and the simulated structure (b).
(c) Time averaged electric field enhancement at y = 0 and z = 0 planes at 633 nm.

3. FABRICATION

We fabricated PCSs with CMOS compatible process which enables future low-cost and large-volume manufacturing. The fabrication flow is illustrated in Fig. 2. In brief, the fabrication starts with creating a two-dimensional ordered array of nanoholes on a 230 nm thick Si_3N_4 film, which is deposited on a fused silica substrate, via EBL followed by reactive ion etching (RIE).

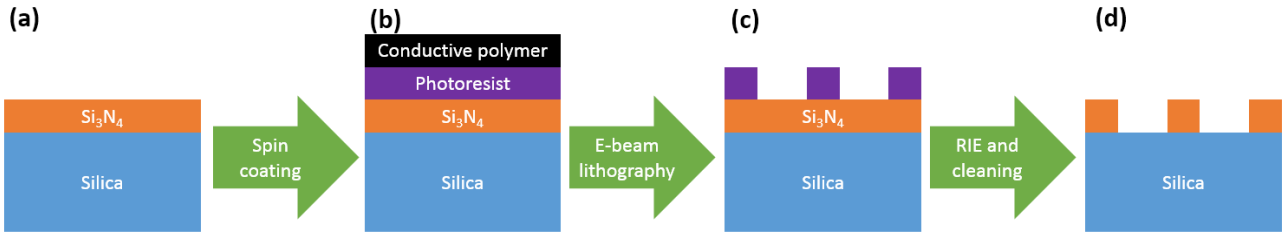

Fig. 2. Fabrication flow of a PCS.

The SERS-active NC-AgNPs are obtained by chemical synthesis including electrochemical deposition and hydrothermal growth [31, 51]. The NCs consist of a tri-layer structure with an Au nanorod as the core, a thin silica layer coated on the surface of the Au core, and an outer layer of high-density Ag NPs grown on the silica layer (Fig. 3(a)).The inner gold nanorod cores are fabricated by electrochemical deposition into nanoporous templates. Billions of nanorods can be made at a time with tunable lengths and diameters [52]. They can be electrically polarized and manipulated in an electric field [53]. The silica layers are synthesized via hydrolysis of tetraethyl orthosilicate (TEOS, 0.8 ml, Alfa Aesar, 99.999+%) in a mixed solution of ammonia (0.2 ml, Fisher Scientific, Certified A.C.S. Plus), ethanol (3 ml, Pharmco-aaper, ACS/USP grade), and Deionized water (1.8 ml), which not only provide supporting substrates for the growth of Ag NPs but also effectively separate them from the Au cores to avoid the possible optical quenching effect. The uniform Ag NPs on the silica surface are grown by the reduction of silver nitrate ($AgNO_3$) in polyvinylpyrrolidone (PVP). The size of Ag NPs and their junctions are optimized to 26 ± 5 nm and 1.8 ± 0.4 nm, respectively, which provide an EF of 3.7×10^8 for ultra-sensitivity SERS detection[54]. Next, the chemically synthesized plasmonic nanocapsules are assembled onto arrays on the lithographed. A typical SEM of a nanocapsule sitting on PCS is shown in Fig. 3(b).

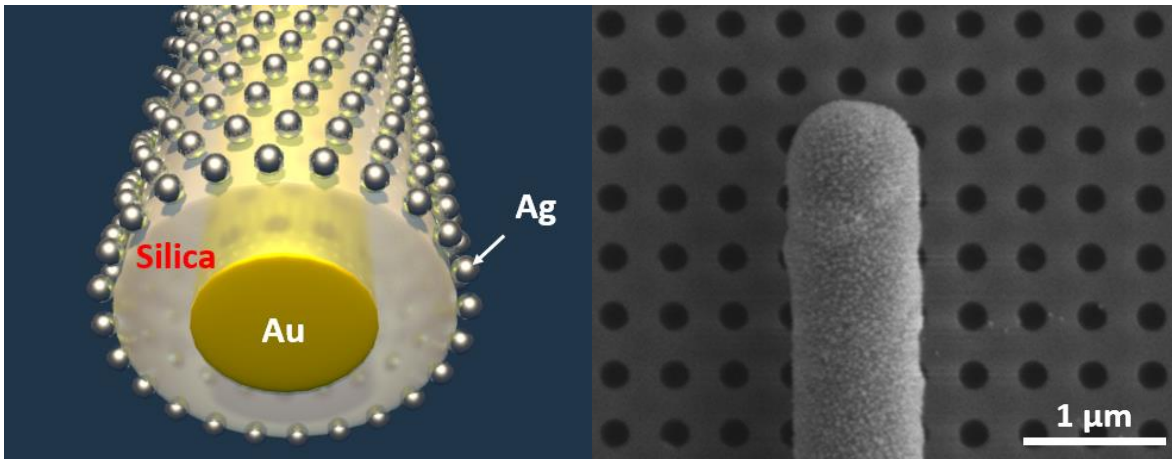

Fig. 3. (a)Cross-sectional 3D schematic diagram of a nanocapsule where a metallic Au nanowire serves as the core, a silica layer grown on the surface of the metal core support the Ag NPs growth, and Ag NPs grow uniformly on the silica layer. (b) Typical SEM image of a nanocapsule sitting on PCS

4. RAMAN SCATTERING MEASUREMENT

The Raman signals are collected both from NC-AgNPs on PCS (device group) and from the ones on reference substrates which is a 230 nm thick Si_3N_4 layer on silica substrate without air holes (control group). Figure 4a shows typical Raman spectra of 10 nM Nile blue from device group (in red) and control group (in black), where the Raman modes are label according to the previous study [55]. The statistic absolute intensities of seven major Raman modes [56] (597 cm^{-1}, 1187 cm^{-1}, 1356 cm^{-1}, 1429 cm^{-1}, 1491 cm^{-1}, 1545 cm^{-1}, and 1642 cm^{-1}) are summarized in Fig. 4b. Due to the GMR from the PCS, we have achieved a further enhancement of 5.11 of the mode at 597 cm^{-1} and a mean enhancement of the other seven major modes of 4.67 times, which results in the total EF factor of this DR-SERS substrate as high as 1.8×10^9.

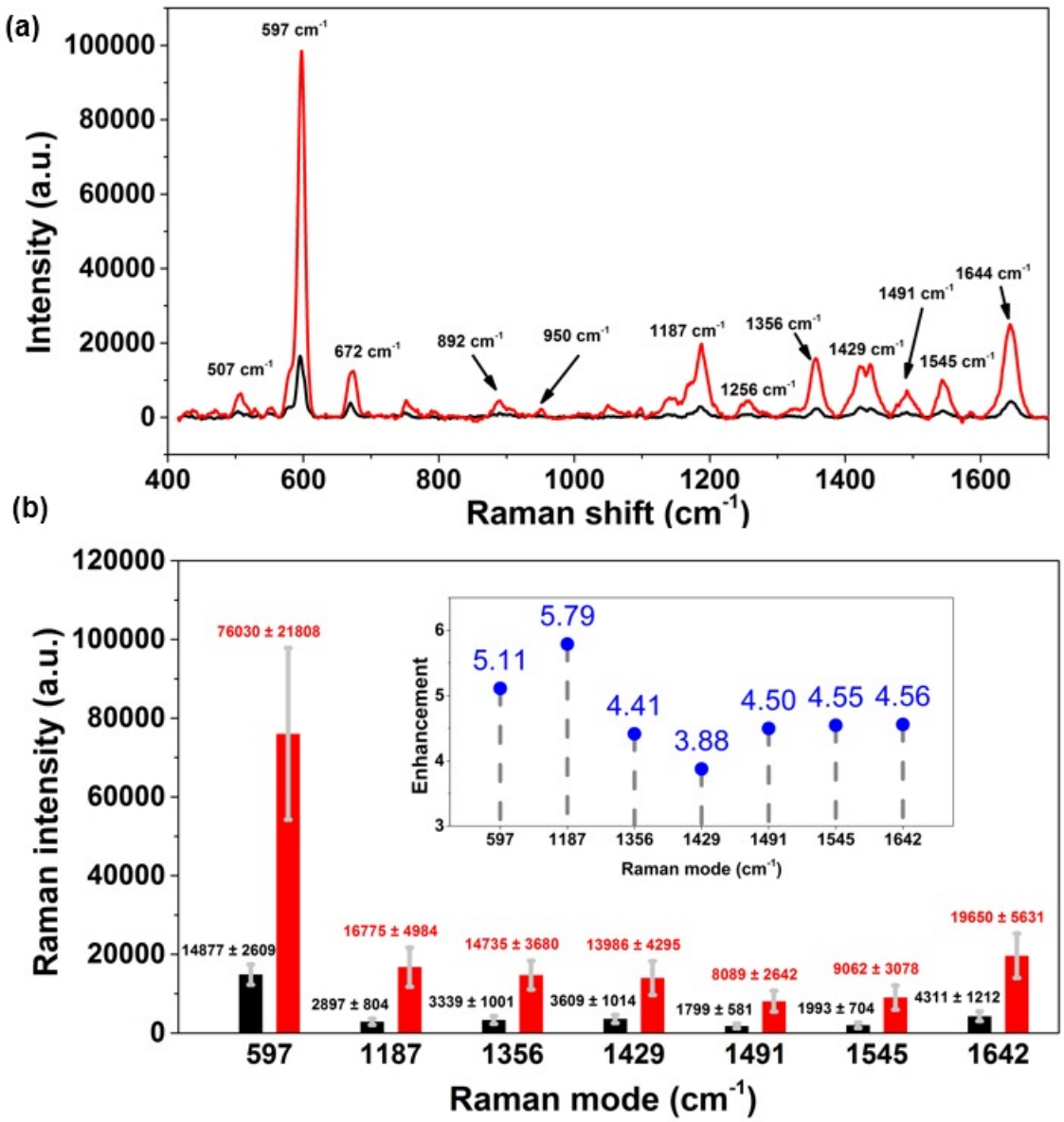

Fig. 4. (a) Typical Raman spectra from NC-AgNPs on the reference substrate (black) and the PCS(red). (b) The statistic Raman intensity of different Raman modes. Inset: Enhancements of the different Raman modes

5. CONCLUSION

In summary, we designed and successfully demonstrated an original type of Raman nanosensors by manipulating and integrating chemically synthesized plasmonic nanocapsules on lithographically patterned PCSs. The photonic crystal can enhance Raman signals by 4.67 times due to the GMR effect, resulting in a robust 1.8×10^9 EF. This work points toward a rational approach to designing future SERS nanosensing devices with ultra-high sensitivity and efficiency for practical applications.

ACKNOWLEDGEMENT

The authors are grateful for the support of National Institutes of Health (NIH) (Grant No. 9R42ES024023-02 and 5R42ES024023-03) and Welch Foundation (Grant No. F-1734).

REFERENCES

[1] C. V. Raman, and K. S. Krishnan, "A new radiation," Indian Journal of Physics, 2, 387-398 (1928).
[2] G. Landsberg, and L. Mandelstam, "Eine neue Erscheinung bei der Lichtzerstreuung in Krystallen," Naturwissenschaften, 16(28), 557-558 (1928).
[3] H. J. Bowley, D. L. Gerrard, J. D. Louden *et al.*, [Practical raman spectroscopy] Springer Science & Business Media, (2012).
[4] D. A. Long, "Raman spectroscopy," New York, 1-12 (1977).
[5] F. Adar, M. Delhaye, and E. DaSilva, "Evolution of instrumentation for detection of the Raman effect as driven by available technologies and by developing applications," Journal of Chemical Education, 84(1), 50-60 (2007).
[6] M. Fleischmann, P. J. Hendra, and Mcquilla.Aj, "Raman-Spectra of Pyridine Adsorbed at a Silver Electrode," Chemical Physics Letters, 26(2), 163-166 (1974).
[7] D. L. Jeanmaire, and R. P. Vanduyne, "Surface Raman Spectroelectrochemistry .1. Heterocyclic, Aromatic, and Aliphatic-Amines Adsorbed on Anodized Silver Electrode," Journal of Electroanalytical Chemistry, 84(1), 1-20 (1977).
[8] M. G. Albrecht, and J. A. Creighton, "Anomalously Intense Raman-Spectra of Pyridine at a Silver Electrode," Journal of the American Chemical Society, 99(15), 5215-5217 (1977).
[9] S.-Y. Ding, J. Yi, J.-F. Li *et al.*, "Nanostructure-based plasmon-enhanced Raman spectroscopy for surface analysis of materials," Nature Reviews Materials, 1, 16021 (2016).
[10] L. D. Qin, S. L. Zou, C. Xue *et al.*, "Designing, fabricating, and imaging Raman hot spots," Proceedings of the National Academy of Sciences of the United States of America, 103(36), 13300-13303 (2006).
[11] K. A. Willets, and R. P. Van Duyne, "Localized surface plasmon resonance spectroscopy and sensing," Annual Review of Physical Chemistry, 58, 267-297 (2007).
[12] A. X. Wang, and X. M. Kong, "Review of Recent Progress of Plasmonic Materials and Nano-Structures for Surface-Enhanced Raman Scattering," Materials, 8(6), 3024-3052 (2015).
[13] J. P. Camden, J. A. Dieringer, Y. M. Wang *et al.*, "Probing the structure of single-molecule surface-enhanced Raman scattering hot spots," Journal of the American Chemical Society, 130(38), 12616-+ (2008).
[14] K. Kneipp, Y. Wang, H. Kneipp *et al.*, "Single molecule detection using surface-enhanced Raman scattering (SERS)," Physical Review Letters, 78(9), 1667-1670 (1997).
[15] S. M. Nie, and S. R. Emery, "Probing single molecules and single nanoparticles by surface-enhanced Raman scattering," Science, 275(5303), 1102-1106 (1997).
[16] B. Pettinger, G. Picardi, R. Schuster *et al.*, "Surface enhanced Raman spectroscopy: Towards single molecular spectroscopy," Electrochemistry, 68(12), 942-949 (2000).
[17] S. Cervo, E. Mansutti, G. Del Mistro *et al.*, "SERS analysis of serum for detection of early and locally advanced breast cancer," Analytical and Bioanalytical Chemistry, 407(24), 7503-7509 (2015).

[18]J. Li, Z. Skeete, S. Y. Shan *et al.*, "Surface Enhanced Raman Scattering Detection of Cancer Biomarkers with Bifunctional Nanocomposite Probes," Analytical Chemistry, 87(21), 10698-10702 (2015).
[19]U. S. Dinish, G. Balasundaram, Y. T. Chang *et al.*, "Actively Targeted In Vivo Multiplex Detection of Intrinsic Cancer Biomarkers Using Biocompatible SERS Nanotags," Scientific Reports, 4, (2014).
[20]Q. An, P. Zhang, J. M. Li *et al.*, "Silver-coated magnetite-carbon core-shell microspheres as substrate-enhanced SERS probes for detection of trace persistent organic pollutants," Nanoscale, 4(16), 5210-5216 (2012).
[21]C. Y. Wen, F. Liao, S. S. Liu *et al.*, "Bi-functional ZnO-RGO-Au substrate: photocatalysts for degrading pollutants and SERS substrates for real-time monitoring," Chemical Communications, 49(29), 3049-3051 (2013).
[22]Y. J. Ye, J. Chen, Q. Q. Ding *et al.*, "Sea-urchin-like Fe3O4@C@Ag particles: an efficient SERS substrate for detection of organic pollutants," Nanoscale, 5(13), 5887-5895 (2013).
[23]J. Y. Xu, J. Wang, L. T. Kong *et al.*, "SERS detection of explosive agent by macrocyclic compound functionalized triangular gold nanoprisms," Journal of Raman Spectroscopy, 42(9), 1728-1735 (2011).
[24]P. R. Sajanlal, and T. Pradeep, "Functional hybrid nickel nanostructures as recyclable SERS substrates: detection of explosives and biowarfare agents," Nanoscale, 4(11), 3427-3437 (2012).
[25]A. Hakonen, P. O. Andersson, M. S. Schmidt *et al.*, "Explosive and chemical threat detection by surface-enhanced Raman scattering: A review," Analytica Chimica Acta, 893, 1-13 (2015).
[26]Y. Shuai, D. Zhao, A. Singh Chadha *et al.*, "Coupled double-layer Fano resonance photonic crystal filters with lattice-displacement," Applied Physics Letters, 103(24), 241106 (2013).
[27]S. S. Wang, and R. Magnusson, "THEORY AND APPLICATIONS OF GUIDED-MODE RESONANCE FILTERS," Applied Optics, 32(14), 2606-2613 (1993).
[28]K. B. Crozier, V. Lousse, O. Kilic *et al.*, "Air-bridged photonic crystal slabs at visible and near-infrared wavelengths," Physical Review B, 73(11), 115126 (2006).
[29]M. Tabatabaei, M. Najiminaini, K. Davieau *et al.*, "Tunable 3D Plasmonic Cavity Nanosensors for Surface-Enhanced Raman Spectroscopy with Sub-femtomolar Limit of Detection," ACS Photonics, 2(6), 752-759 (2015).
[30]E. Le Ru, and P. Etchegoin, [Principles of Surface-Enhanced Raman Spectroscopy: and related plasmonic effects] Elsevier, (2008).
[31]X. Xu, K. Kim, C. Liu *et al.*, "Fabrication and Robotization of Ultrasensitive Plasmonic Nanosensors for Molecule Detection with Raman Scattering," Sensors, 15(5), 10422 (2015).
[32]A. Wang, and X. Kong, "Review of Recent Progress of Plasmonic Materials and Nano-Structures for Surface-Enhanced Raman Scattering," Materials, 8(6), 3024 (2015).
[33]L. Chen, H. J. Yang, Z. X. Qiang *et al.*, "Colloidal quantum dot absorption enhancement in flexible Fano filters," Applied Physics Letters, 96(8), (2010).
[34]F. S. Ou, M. Hu, I. Naumov *et al.*, "Hot-Spot Engineering in Polygonal Nanofinger Assemblies for Surface Enhanced Raman Spectroscopy," Nano Letters, 11(6), 2538-2542 (2011).
[35]X. B. Xu, D. H. Hasan, L. Wang *et al.*, "Guided-mode-resonance-coupled plasmonic-active SiO_2 nanotubes for surface enhanced Raman spectroscopy," Applied Physics Letters, 100(19), 191114 (2012).
[36]X. B. Xu, H. F. Li, D. Hasan *et al.*, "Near-Field Enhanced Plasmonic-Magnetic Bifunctional Nanotubes for Single Cell Bioanalysis," Advanced Functional Materials, 23(35), 4332-4338 (2013).
[37]X. B. Xu, K. Kim, and D. L. Fan, "Tunable Release of Multiplex Biochemicals by Plasmonically Active Rotary Nanomotors," Angewandte Chemie-International Edition, 54(8), 2525-2529 (2015).
[38]C. Liu, X. Xu, and D. L. Fan, "Electric-Field Enhanced Molecule Detection in Suspension on Assembled Plasmonic Arrays by Raman Spectroscopy," Journal of Nanotechnology in Engineering and Medicine, 5(4), 040906-040906 (2014).
[39]V. Liu, and S. H. Fan, "S-4: A free electromagnetic solver for layered periodic structures," Computer Physics Communications, 183(10), 2233-2244 (2012).
[40]O. Kilic, S. Kim, W. Suh *et al.*, "Photonic crystal slabs demonstrating strong broadband suppression of transmission in the presence of disorders," Optics Letters, 29(23), 2782-2784 (2004).
[41]Y. C. Shuai, D. Y. Zhao, A. S. Chadha *et al.*, "Coupled double-layer Fano resonance photonic crystal filters with lattice-displacement," Applied Physics Letters, 103(24), (2013).
[42]Y. C. Shuai, D. Y. Zhao, Z. B. Tian *et al.*, "Double-layer Fano resonance photonic crystal filters," Optics Express, 21(21), 24582-24589 (2013).
[43]Y. H. Liu, A. Chadha, D. Y. Zhao *et al.*, "Approaching total absorption at near infrared in a large area monolayer graphene by critical coupling," Applied Physics Letters, 105(18), (2014).

[44]D. Zhao, H. Yang, J.-H. Seo *et al.*, "Design and Characterization of Photonic Crystal Membrane Reflector Based Vertical Cavity Surface Emitting Lasers on Silicon," Reviews in Nanoscience and Nanotechnology, 3(2), 77-87 (2014).
[45]R. Gad, W. T. Lau, C. Nicholaou *et al.*, "Tailoring of spectral response and spatial field distribution with corrugated photonic crystal slab," Optics Letters, 40(16), 3715-3718 (2015).
[46]V. K. Narasimhan, T. M. Hymel, R. A. Lai *et al.*, "Hybrid Metal–Semiconductor Nanostructure for Ultrahigh Optical Absorption and Low Electrical Resistance at Optoelectronic Interfaces," ACS Nano, 9(11), 10590-10597 (2015).
[47]Y. L. Xu, T. Gong, and J. N. Munday, "The generalized Shockley-Queisser limit for nanostructured solar cells," Scientific Reports, 5, (2015).
[48]J. R. Piper, and S. H. Fan, "Broadband Absorption Enhancement in Solar Cells with an Atomically Thin Active Layer," Acs Photonics, 3(4), 571-577 (2016).
[49]E. C. Regan, Y. C. Shen, J. J. Lopez *et al.*, "Substrate-Independent Light Confinement in Bioinspired All Dielectric Surface Resonators," Acs Photonics, 3(4), 532-536 (2016).
[50]A. Yang, K. Yang, H. Yu *et al.*, "Piezoelectric tuning of narrowband perfect plasmonic absorbers via an optomechanic cavity," Optics Letters, 41(12), 2803-2806 (2016).
[51]X. B. Xu, K. Kim, H. F. Li *et al.*, "Ordered Arrays of Raman Nanosensors for Ultrasensitive and Location Predictable Biochemical Detection," Advanced Materials, 24(40), 5457-5463 (2012).
[52]T. M. Whitney, J. S. Jiang, P. C. Searson *et al.*, "Fabrication and Magnetic-Properties of Arrays of Metallic Nanowires," Science, 261(5126), 1316-1319 (1993).
[53]D. L. Fan, F. Q. Zhu, R. C. Cammarata *et al.*, "Electric tweezers," Nano Today, 6(4), 339-354 (2011).
[54]C. Liu, Z. Wang, E. Li *et al.*, "Electrokinetic Manipulation Integrated Plasmonic–Photonic Hybrid Raman Nanosensors with Dually Enhanced Sensitivity," ACS Sensors, (2017).
[55]S. K. Miller, A. Baiker, M. Meier *et al.*, "Surface-enhanced Raman scattering and the preparation of copper substrates for catalytic studies," Journal of the Chemical Society, Faraday Transactions 1: Physical Chemistry in Condensed Phases, 80(5), 1305-1312 (1984).
[56]M. K. Lawless, and R. A. Mathies, "Excited‐state structure and electronic dephasing time of Nile blue from absolute resonance Raman intensities," The Journal of chemical physics, 96(11), 8037-8045 (1992).